

## Sensitive Electrocatalytic Assay of Cyclotetramethylene Tetranitramine (HMX) Explosive on Carbon Nanotube/Ag Nanocomposite Electrode

Sajjad Damiri\*, Hamid Reza Pouretedal, Maryam Mahmoudi

Department of Applied Chemistry, Maleke-ashtar University of Technology, Shahin-shahr, Esfahan, Iran

Received 25 April 2021; received in revised form 7 February 2022; accepted 11 February 2022

### ABSTRACT

An efficient electrocatalyst was developed based on silver nanoparticles/multi walled carbon nanotubes nanocomposite modified glassy carbon electrode (AgNPs/MWCNTs/GCE) by controlled electrodeposition and continuous double-potential pulses to test the high explosive cyclotetramethylene-tetranitramine (HMX) using cyclic voltammetry method. The electrochemical behavior of the system in various pHs was studied by cyclic voltammetry (CV), electrochemical impedance spectroscopy (EIS), chronoamperometry and chronocoulometry; and some reduction parameters, including the transfer coefficient ( $\alpha$ ), electron transfer number, apparent electron transfer rate, and diffusion coefficient constants of HMX were estimated. The results demonstrated that reduction of HMX by adsorptive stripping voltammetry on AgNPs/MWCNTs film could remarkably be enhanced and catalyzed compared to bare carbon nanotubes electrode, and the reduction potential could be facilitated from -0.7 V (vs. SCE) to -0.3 V, with electron exchange rate constant of  $1.12 \pm 0.1 \text{ s}^{-1}$  and  $0.17 \pm 0.1 \text{ s}^{-1}$  for AgNPs/MWCNTs and bare MWCNTs electrodes. Chronoamperometry studies showed a diffusion-controlled process with an apparent diffusion coefficient of  $2.01 \times 10^{-4} \text{ cm}^2 \text{ s}^{-1}$  and a catalytic rate constant of 7.48 times higher than that of bare MWCNTs electrode. Also, chronocoulometric studies showed that the number of electrons transferred for electrochemical reduction of HMX was near 1.98. Under optimized conditions, the reduction peak had two linear dynamic ranges of 2.0-30.0 and 30.0-120.0  $\mu\text{M}$  with the experimental detection limit of 0.2  $\mu\text{M}$  and precision of <2.5% (RSD for five analyses). This modified electrode can be properly used to determine HMX in soil and groundwater samples with satisfactory results.

**Keywords:** HMX Explosive; Carbon nanotubes; Silver nanoparticles; Voltammetry; Determination.

### 1. Introduction

Cyclotetramethylene-tetranitramine (HMX or High Melting point Explosive), commonly called Octogen, is one of the strongest military explosives due to its high detonation velocity and thermal stability, which is used commonly in various energetic materials of ammunition, rocket, and missile warheads [1]. HMX, having a nitramine functional group, has a chemical behavior similar to its similar homolog cyclotrimethylenetrinitramine (RDX), but, unexpectedly, in electrochemical detections, it does not show a good current signal [2]. Of course, HMX in solid-state has four polymorphic types of  $\alpha$ ,  $\beta$ ,  $\gamma$  and  $\delta$ , which differ in terms of density and sensitivity to physical initiators, such as impact and friction [3,4].

According to military specification [5,6], only  $\beta$ -HMX, having more safety and density, should be used in standard military energetic materials.

Today, the selective and sensitive detection of various energetic materials, such as HMX, is the main approach for efficiently determining explosive pollutants in various environmental and military samples. By reviewing scientific publications, the following reports are provided for the detection or measurement of HMX in different environments: Fourier transform infrared spectroscopy (FT-IR) and high-performance liquid chromatography (HPLC) for determination of HMX and RDX in explosive compounds [7], HPLC coupled to electrospray ionization mass spectrometry (ESI-MS) for quantitative analysis of HMX in environmental samples in the concentration linear range of 5.0-50  $\mu\text{g/L}$  [8], an square wave voltammetry (SWV) technique on glassy carbon electrode (GCE) at relatively expensive and hazardous organic media for the electrochemical

\*Corresponding author:

E-mail address: [s\\_damiri@mut-es.ac.ir](mailto:s_damiri@mut-es.ac.ir) (S. Damiri)

reduction of RDX and HMX in soil samples [9], HPLC with ultraviolet (UV) detector for the separation and determination of various explosives containing HMX with the limit of detection (LOD) near to 0.09  $\mu\text{g/L}$  [10], a 4-aminothiophenol functionalized gold nanoparticle-based colorimetric sensor for determination of nitramine energetic materials with LOD of 0.24 ppm for HMX [11], an UV spectroscopy method for simultaneous determination of trinitrotoluene (TNT), RDX, and HMX [12], a boron-doped graphene modified GCE for electrochemical reduction study and determination of HMX by cyclic voltammetry (CV) with LOD near to 245.8 ppb were used [13].

The use of unique electrochemical methods with some characteristics, such as portability, low cost, high sensitivity, fast detection, and various diagnostic techniques and electrocatalytic modified electrodes, is an appropriate approach for inexpensive and fast field detection of explosives [14-16]. Although HMX has four reducible nitramine functional groups, unlike RDX, the reduction signal of HMX is extremely weak on the conventional electrodes [2], and the scientific reports on this compound are limited.

This work aims to develop a sensitive electro-reduction route for the detection of HMX explosives in water conditions, based on the specific and synergetic properties of MWCNTs and nanostructured Ag nanocomposite as a working electrode, having excellent electrocatalytic activity, high specific area, and strong adsorptive ability. The modification of electrode substrates with carbon nanotubes has been reported to result in the low detection limits, high sensitivities, reduction of overpotentials, and resistance to surface fouling [14]. Also, nanostructured Ag semiconductors have long-term stability, low cost, and useful electrocatalytic activities [17]. The proposed method provides some advantages, such as high electrocatalytic activity, rapid response, low cost, and simplicity, which is promising for determining HMX explosive contamination in some environmental samples, including soil and groundwater.

## 2. Experimental

### 2.1. Chemicals

All used chemicals, such as dimethylformamide (DMF) solvent, potassium di-hydrogen phosphate, silver nitrate, etc., were analytical reagent grade purchased from Merck (Darmstadt, Germany) unless otherwise stated. Explosive materials, such as HMX and RDX with purity >99.8 wt. % was purchased from Iranian defense industries. Buffer solutions of 0.1-0.8 M were prepared by potassium di-hydrogen phosphate and

potassium hydroxide solution, with standard calibrants. 2.0 mM mother liquor of HMX was prepared by dissolving 0.05923 g HMX in 100 mL DMF solvent, and more diluted solutions were prepared by mixing mother liqueur and distilled water.

Caution: All explosives, such as HMX, are dangerous and must be carefully handled and used following approved safety procedures either by or under the direction of competent, experienced persons in accordance with all applicable laws and regulations.

### 2.2. Apparatus

All electrochemical experiments were carried out by a conventional three-electrode cell powered by SAMA-500 electrochemical system and Behpajoo Co. software. Electrochemical impedance spectroscopy (EIS) studies were performed using an Autolab system with FRA2 boards (Eco Chemie B. V., Utrecht, Netherlands) and FRA 4.9. The three-electrode cell assembly consists of a graphite wire as an auxiliary electrode, a saturated Calomel electrode (SCE) as a reference electrode, and MWCNTs or AgNPs/MWCNTs/GCE electrode as a working electrode. Also, a Corning M140 PH-meter with a double junction glass electrode was used for preparing buffer electrolytes. Nanocomposites layers were characterized using scanning electron microscopy (SEM), Philips XI-300 equipped with energy-dispersive X-ray analyzer (EDAX).

### 2.3. Preparation of modified electrode

Low HMX concentration (< 1.0 mM) on GCE and MWCNTs shows an extremely weak reduction signal or electron transfer kinetics. To increase the sensor's sensitivity, GCE was modified by MWCNTs similar to [18] so that the Ag nanoparticles were electrodeposited on its surface. Here carbon nanotubes were functionalized and dis-aggregated in an organic solvent, then it was deposited and dried on the electrode. Thereafter, a 1.0 mM solution of silver nitrate was prepared at pH=3, and Ag nanoparticles were deposited on MWCNTs surface, using a continuous pulse potential route [19]. A double-potential pulse sequence with cathodic pulse potentials of -0.5 V at a pulse time interval of 5 seconds, the anodic potential of 0.0 V at relaxation time of 20 seconds, and pulse numbers of 50 times were continuously applied and optimized. By these potential cycling, a deposition-dissolution mechanism occurs for Ag nanoparticles and creates a thin Ag film on the MWCNTs surface. The microscopic areas of the MWCNT-modified GCE and the bare GCE were obtained by cyclic voltammetry using 1 mM

$K_3Fe(CN)_6$  as a probe at different scan rates probe and different scan rates [14,20]. The microscopic surface area of bare GCE, MWCNT, and AgNPs/MWCNTs electrodes was found to be 0.0314, 0.0610, and 0.0704  $cm^2$ , respectively.

#### 2.4. Electrochemical studies

The electrochemical behavior of HMX was studied using the cyclic voltammetry technique. 10.0 mL single standard solution of 10.0  $\mu M$  HMX was prepared in water containing 0.1 M buffer solution with pH 3.0 as a supporting electrolyte. The peak current ( $I_p$ ), peak potential ( $E_p$ ), and some electroreduction parameters were evaluated. In reduction voltammetry studies, the electrochemical cell was de-oxygenated and stirred with nitrogen gas at the desired accumulation potential for a given period of time to pre-concentrate the analyte on the working electrode surface. Stirring was then stopped, the solution was allowed to rest for 60.0 seconds, and the electrode potential was scanned between 0.0 and -1.0 V, and other settings. After each measurement, a new electrode surface was obtained by slightly rinsing with acetone/methanol solution and water.

#### 2.5. Preparation and analysis of real samples

A given amount of HMX solution was added to the soil and ground real samples, and the recovery percent of the analyte concentration was experimentally obtained by cyclic voltammetry at pH 3.0. Then, 0.625 and 1.250 mL of HMX solution was added to 10.0 g of soil samples, followed by extracting the explosive contaminants of the homogenized sample using 200.0 mL DMF solvent for 3 times. The sediment in the extracts was separated by centrifugation with a volume of 250.0 mL. For electrochemical tests, 1.0 mL of these samples were diluted to 10.0 mL with a 5.0 mL buffer solution with pH 3.0 and water. Also, 4.0 mL groundwater samples (from Isfahan, Shahin-Shahr) were spiked with HMX solution and diluted to 10.0 mL with 5.0 mL of 0.1 M buffer solution and water. All experiments were carried out by cyclic voltammetry from 0.0 to -1.2 V and 100.0  $mV s^{-1}$  potential scan rate.

### 3. Results and Discussion

#### 3.1. Voltammetry and EIS studies of HMX on AgNPs/MWCNTs nanocomposite electrode

Typical SEM images of AgNPs/MWCNTs electrodes are shown in Fig. 1. As shown in the figure, silver nanoparticles deposit in the size range of 10-200 nm uniformly on the surface of carbon nanotubes. Also,

elemental analysis by X-ray dispersion (EDAX) method shows the presence of silver elements on the electrode surface.

Fig. 2 shows the cyclic voltammograms of 10.0  $\mu M$  HMX analysis on the surface of two working MWCNTs-modified GCE and AgNPs/MWCNTs/GCE electrodes. No significant current signal is observed on the bare carbon nanotube electrode for electrochemical reduction of nitramine functional groups of 10.0  $\mu M$  HMX. HMX reduction on the surface of AgNPs/MWCNTs nanocomposite is significantly facilitated by a synergetic effect, and the reduction potential is started near to -0.3 V, showing a unique electrocatalytic effect of the mentioned electrocatalyst. It seems that the highly reactive nature of nanomaterial dominated by a large percentage of high-energy surface Ag atoms with low lattice co-ordination number [21], and accumulation of HMX on the high-specific surface area of AgNPs/MWCNTs, along with the presence of extremely high edges and defects on this modified electrode lead to significant enhancement of the HMX cathodic current [17].

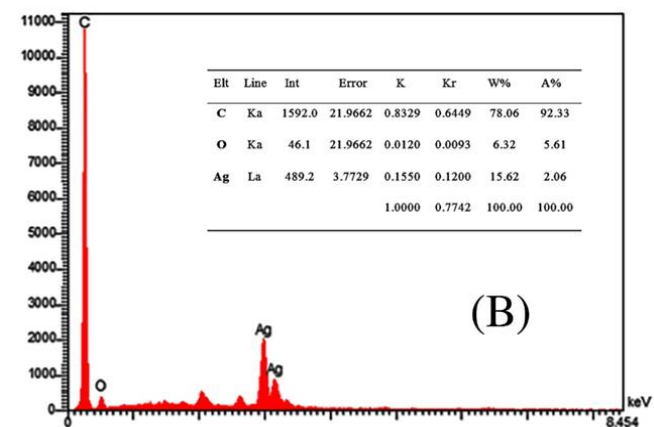
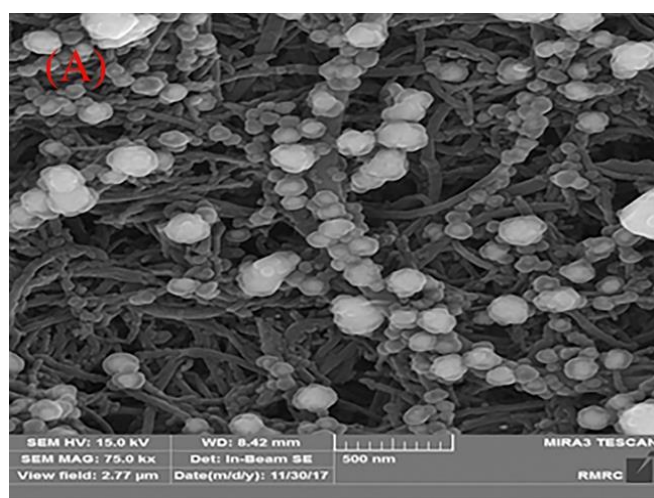


Fig. 1. A) Typical SEM images and B) Energy dispersive X-ray elemental analysis of AgNPs/MWCNTs nanocomposite.

As depicted in **Fig. 3** for EIS studies, the Nyquist diagram of 10.0  $\mu\text{M}$  HMX on AgNPs/MWCNTs nanocomposite and bare MWCNTs-modified GCE electrodes at -0.5 V represent one slightly depressed capacitive semicircle at high frequencies related to the charge-transfer resistance and double-layer capacitance. Equation (1) explain the relationship between apparent electron transfer rate constant ( $k_{app}$ ) and the electron transfer resistance ( $R_{ct}$ ) on Nyquist diagrams and concentration of HMX ( $\text{mol cm}^{-3}$ ) [22]:

$$k_{app} = \frac{RT}{n^2 F^2 A R_{ct} C} \quad (1)$$

where  $n$  is the number of transferred electrons ( $n=2$ ),  $A$  is the microscopic area of the electrodes,  $R$ ,  $T$ , and  $F$  have their usual meanings.

The equivalent circuits compatible with the Nyquist diagrams recorded for the two electrodes are depicted in the inset of **Fig. 3**. The equivalent model circuits contain the solution resistance ( $R_s$ ), the charge-transfer resistance ( $R_{ct}$ ), and a constant phase element corresponding to the double-layer capacitance ( $CPE_{dl}$ ). Also,  $W$ , which is included in the circuit, is the Warburg element related to the semi-infinite diffusion process. The impedance of CPE and  $W$  can be expressed as [23]:

$$Z_{CPE} = (Y_0 j \omega)^{-n} \quad (2)$$

$$Z_W = Y_0^{-1} (j \omega)^{-1/2} \quad (3)$$

where  $Y_0$  (the admittance parameter,  $\text{S cm}^{-2} \text{s}^{-n}$ ) and  $n$  (dimensionless exponent) are two parameters independent of frequency;  $j = (-1)^{1/2}$ , and  $\omega$  is angular frequency  $= 2\pi f$ .

The equivalent circuit elements obtained by fitting the experimental results shows  $R_{ct}$ , for the 10.0  $\mu\text{M}$  HMX on the bare nanotube electrode and AgNPs/MWCNTs electrode equals to 1356.1 ( $\pm 3.4\%$ ) and 396.7 ( $\pm 2.7\%$ )  $\Omega\text{cm}^2$ , respectively, indicating the much faster charge transfer rate for reduction of HMX on the modified electrode surface. Therefore, the apparent electron transfer rate constant on the AgNPs/MWCNTs electrode, obtained from equation (1), is about 3.42 times higher than that of the bare electrode, demonstrating enhancement of charge transfer reaction kinetics.

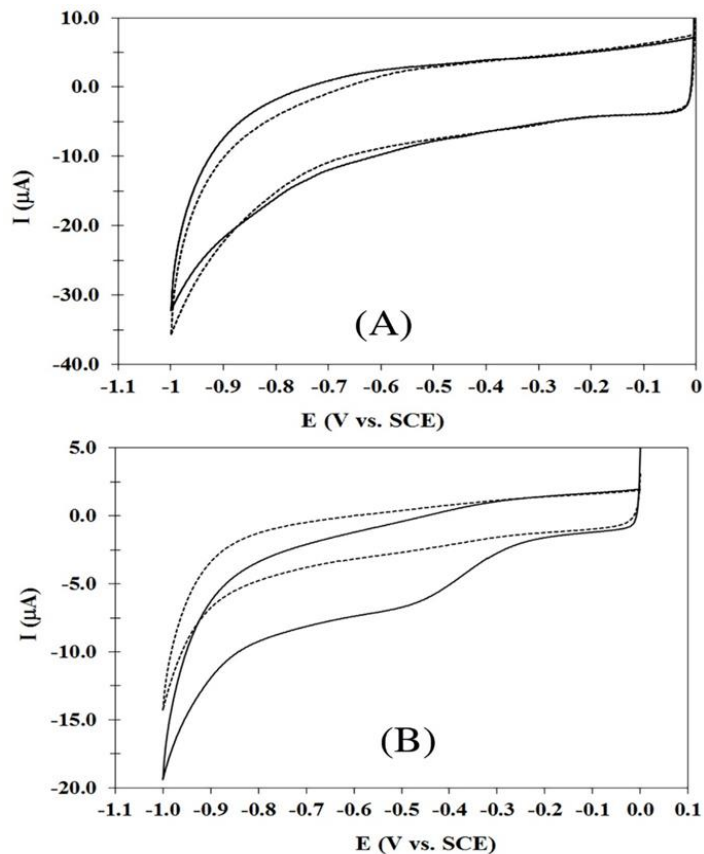


**Fig. 2.** CV voltammograms of 10.0  $\mu\text{M}$  HMX on; A) MWCNTs, and B) AgNPs/MWCNTs nanocomposite electrodes, in the conditions of pH=3.0, phosphate buffer, potential scan rate of 100.0  $\text{mV s}^{-1}$  and nitrogen purging near to 5.0 min. Dashed lines show background signals.

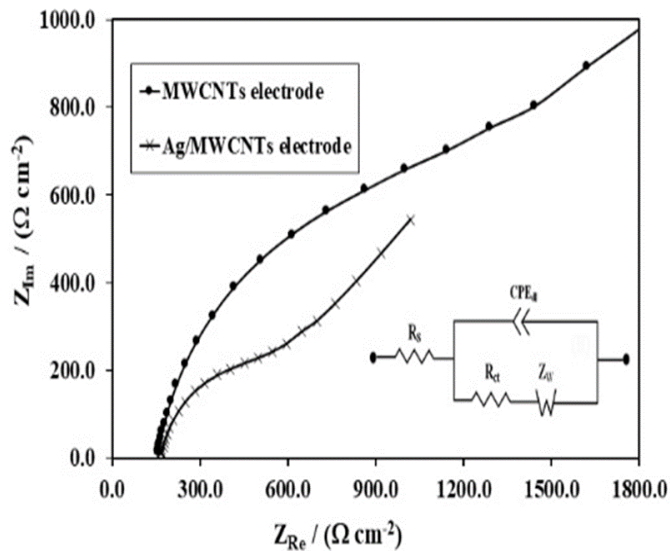


**Fig. 3.** Nyquist plots of EIS studied for the reduction of 10.0  $\mu\text{M}$  HMX on MWCNTs and AgNPs/MWCNTs nanocomposite electrodes at the DC potential of -0.5 mV and phosphate buffer with pH=3.0

### 3.2. Effect of pH on the reduction of HMX

According to the results presented in Fig. 4, the effect of pH on the reduction and potential current of HMX was investigated. It is observed that the highest reduction signal is observed at pH=3.0. Severe reduction of current in alkaline pHs can be due to chemical degradation of HMX. Nitramine explosives such as HMX and RDX do not have suitable stability in alkaline environments and can be destroyed [24]. Also, metal-modified electrodes in those conditions show non-Nernstian behavior, and chemical oxidation causes disorder in electrode responses [17,25]. As seen in Fig. 4, the peak potential of HMX reduction at higher pH is moved towards more negative potentials, indicating hydrogen ion transfer during the electrochemical process[23]. HMX has four nitramine functional groups, with spatial isomerism[3]. As shown in Scheme 1, the reduction mechanism of nitramines in acidic media proceeds via a 2-electron reduction at each nitro group, resulting in the formation of an N-nitroso intermediate, which can be further reduced at more negative potentials to N-amine compounds [2].

Also, the adsorptive stripping and peak currents of 10.0  $\mu\text{M}$  HMX were measured by cyclic voltammetry for 6.0 min accumulation at a different potential from -0.3 to +0.2 V in pH 3.0. It was observed the adsorptive stripping response does not change significantly by accumulation potential (not shown). Thus, further experiments were employed at open circuit potential.

### 3.3. Effect of scan rate on the peak currents and potentials

Cyclic voltammograms of 10.0  $\mu\text{M}$  HMX in pH=3.0 were recorded at various potential scan rates, from 10.0 to 100  $\text{mV s}^{-1}$  (not shown). The cathodic peak current linearly increased with the square root of scan rate, and the following equation was obtained:  $I (\mu\text{A}) = 26.72 v^{1/2} (\text{V s}^{-1}) + 0.32$ ,  $R^2=0.9916$ , that indicates a diffusion-controlled reaction occurring on the electrode[23]. Also, the linear relationship of logarithmic scan rate ( $v$ ) and peak potential ( $E$ ) of an irreversible reaction are based on the following equation[23]:

$$E(V) = E'_0(V) - \frac{RT}{\alpha nF} (V) \left[ 0.780 + \ln \left[ \left( \frac{D_0^{\frac{1}{2}}}{k_0} \right) / (S^{\frac{1}{2}}) \right] + \ln \left[ \left( \frac{\alpha nFv}{RT} \right)^{1/2} / (S^{\frac{1}{2}}) \right] \right] \quad (4)$$

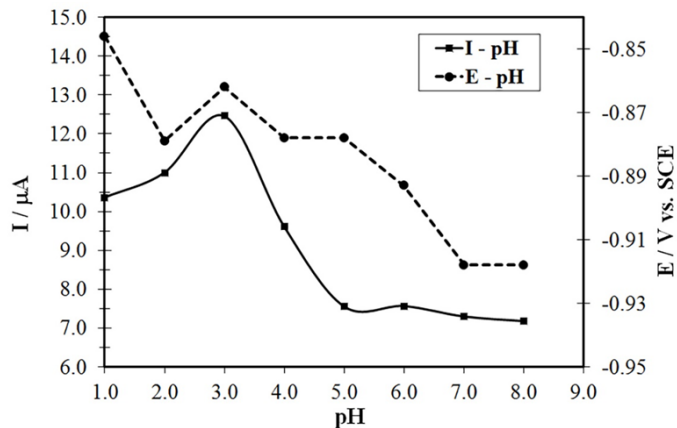
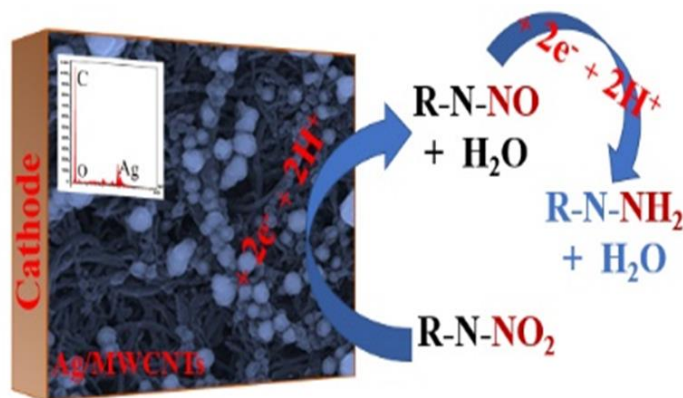


Fig. 4. Electrochemical reduction current and potential changes of 10.0  $\mu\text{M}$  HMX versus pH, and the potential scan rate of 100.0  $\text{mV s}^{-1}$ .



Scheme 1. Proposed diagram showing the reduction process of HMX on AgNPs/MWCNTs nanocomposite electrodes.

where  $E'_0$  is the formal potential,  $n$  presents the number of electrons,  $\alpha$  presents transfer coefficient,  $F$  presents the Faraday constant,  $D_0$  presents the diffusion coefficient,  $k_0$  is the standard heterogeneous rate constant,  $R$  is the gas constant, and  $T$  is the absolute temperature (300 K).

The experimental relationship between the  $E$  and the  $v$  (10.0-100.0  $\text{mV s}^{-1}$ ) shows the equation:  $E(\text{V}) = -0.0899 \times \ln [v (\text{V s}^{-1})] + 0.8642$ ,  $R^2=0.9998$ , and the value of  $\alpha n$  was calculated 0.28. Also, from the slopes ( $E$  vs.  $\log(I_p)$ ), or  $(-\alpha n_\alpha Fv)/2.3RT$  and intercepts ( $\log I_0$ ) of Tafel plots, obtained from background-corrected linear sweep voltammetry experiments at a low scan rate of 5.0  $\text{mV s}^{-1}$  (based on 5.0 replicates) in 10.0  $\mu\text{M}$  concentration of HMX, the mean values of  $\alpha$  and  $K_0$  (exchange rate constant, as a measure of rate reaction) for the AgNPs/MWCNTs (A) and bare MWCNTs electrodes (B) were calculated:  $\alpha_A = 0.27 \pm 0.02$ ,  $K_{0(A)} = 1.12 \pm 0.1 \text{ s}^{-1}$ ,  $\alpha_B = 0.18 \pm 0.02$ , and  $K_{0(B)} = 0.17 \pm 0.1 \text{ s}^{-1}$ , respectively [25-27]. Therefore, the electron exchange rate constant of the modified electrode is

about 6.59 times higher than that of the bare MWCNTs electrode. The obtained  $\alpha$  and  $k_0$  values by LSV and Tafel plots show a good agreement with those obtained in chronoamperometric studies in section 3.5.

### 3.4. Calculation of electron number using chronocoulometry

The large amplitude potential step chronocoulometric method was applied to estimate the number of cathodic electrons exchanged in the reduction reaction of HMX on the modified electrode. Potential steps from 0.0 to -0.7 mV were used, and the signals were recorded for various concentrations of HMX (see Fig. 5). The number of transferred electrons was derived from the forward slope charge value ( $Q_d$ ) of Anson's plot ( $Q$  against  $t^{1/2}$ ) obtained in these experiments using the following equation [ $Q_d = 2nFAD^{1/2}Ct^{1/2}/\pi^{1/2}$ ], where,  $n = \text{eq./mole}$ ,  $F = \text{the Faraday constant (96485)}$ ,  $A = \text{area of the electrode (0.070 cm}^2\text{)}$ ,  $D = \text{diffusion coefficient in cm}^2\text{/s}$ ,  $C = \text{bulk concentration in mol/cm}^3$  and  $t = \text{time in seconds}$ .

The curve of slope vs. HMX concentration show a linear relationship with the following equation; Slope ( $\mu\text{C}\cdot\text{s}^{-1/2}$ ) =  $184.76 C(\mu\text{mol/cm}^3) - 16.47$  or  $2nFAD^{1/2} = 184.76$ . The diffusion coefficient of HMX in water solutions was reported to be  $1.5 \times 10^{-4} \text{ cm}^2 \text{ s}^{-1}$  [26]. Therefore, the number of electrons transferred for the cathodic reaction of HMX on the modified electrode can be estimated near 1.98.

### 3.5. Chronoamperometric studies

For diffusion-controlled reactions, by using the Cottrell equation (Eq. 3), the plot of  $I$  versus  $t^{-1/2}$  will be linear, and from its slope, the value of  $D$  can be calculated [29,30];

$$I = \frac{nFAD_0^{1/2}C^*}{\pi^{1/2}t^{1/2}} \quad (5)$$

As depicted in Fig. 6, the diffusion coefficient of HMX on the modified electrode was studied by chronoamperometry, at a potential step from 0.0 to -0.7 V. According to Cottrell equation, the relevant experimental plots of  $I$  vs.  $t^{-1/2}$  show linear least square fits. The slopes of the resulting straight lines were then plotted versus the HMX concentration with the equation of ; Slope ( $\mu\text{A}\cdot\text{s}^{-1/2}$ ) =  $108.46 C(\mu\text{mol/cm}^3) - 53.53$ , and apparent diffusion coefficient for 2-electrons process was calculated near to  $2.01 \times 10^{-4} \text{ cm}^2 \text{ s}^{-1}$ .

Kinetic studies by chronoamperometry at the potential step of 0.0 to -0.5 V can confirm the electron transfer rate on the bare and modified electrodes. The rate constants are calculated by following equation [23, 30]:

$$\frac{I_C}{I_L} = \gamma^{1/2} \pi^{1/2} = \pi^{1/2} (kC_0 t)^{1/2} \quad (6)$$

where  $I_C$  and  $I_L$  show current in the presence and absence of HMX, and  $\gamma = kC_0 t$  ( $k$  is the catalytic rate constant ( $\text{M}^{-1} \text{ s}^{-1}$ )  $C_0$  is the concentration of HMX, and the time elapsed (s)). At the intermediate time (0.2–1.0 s in the present work), the catalytic current ( $I_C$ ) is dominated by the rate of electrocatalytic reduction of HMX.

The chronoamperometric results (not presented) showed that the apparent  $k$  calculated from the  $I_C/I_L$  vs.  $t^{1/2}$  for 10.0  $\mu\text{M}$  HMX on the bare MWCNTs/GCE and AgNPs/MWCNTs/GCE electrodes are about  $(1.66 \pm 0.12) \times 10^4 \text{ M}^{-1} \text{ s}^{-1}$  and  $(12.42 \pm 0.21) \times 10^4 \text{ M}^{-1} \text{ s}^{-1}$  respectively. Therefore, the catalytic rate constant of HMX on AgNPs/MWCNTs nanocomposite is 7.48 times higher than that of bare MWCNTs.

### 3.6. Performance of sensor for measurement of HMX

Under the optimum conditions of pH 3.0 and a potential scan rate of  $100 \text{ mV s}^{-1}$ , typical cyclic voltammograms of HMX on the modified electrode are presented in Fig 7. Calibration plots (not shown), have two linear dynamic ranges in the concentration region of 2.0-30.0

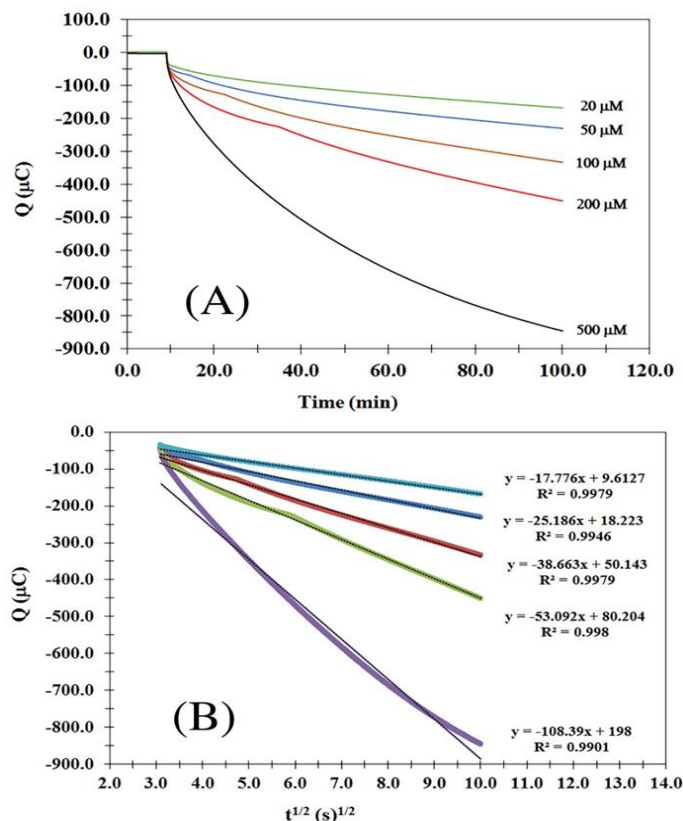
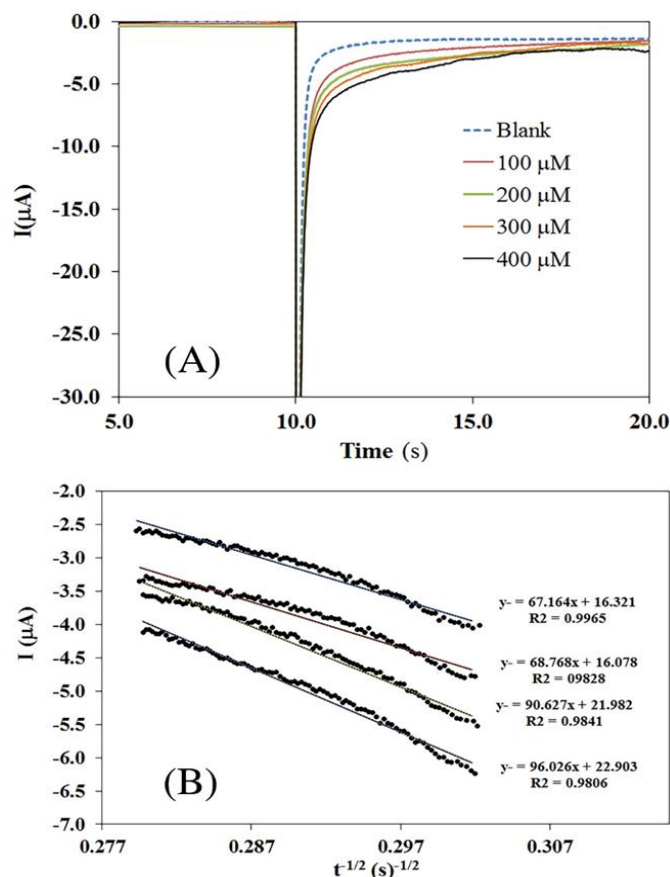
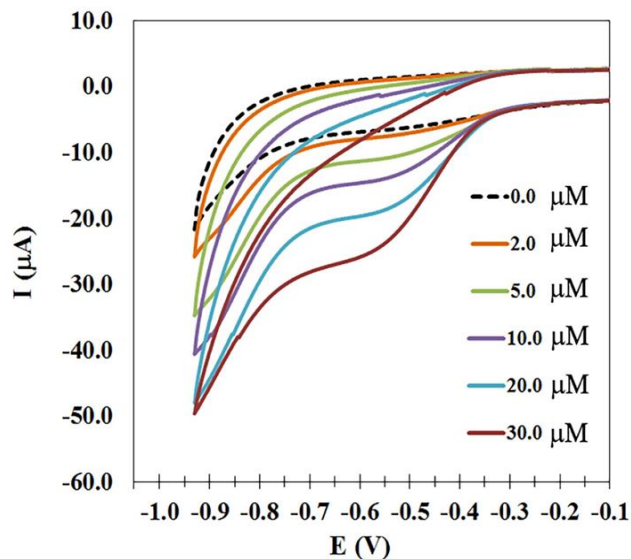


Fig. 5. A) Chronocoulometric curves and B) linear relationship of  $Q$  vs.  $t^{1/2}$  data for various concentrations of HMX at potential steps from 0.0 to -0.7 mV and pH=3.0.



**Fig. 6.** A) Chronoamperometric curves and B) linear relationship of current vs.  $t^{-1/2}$  data for various concentrations of HMX at potential steps from 0.0 to -0.7 mV and pH=3.0.



**Fig. 7.** A typical CV voltammograms of various concentration of HMX at phosphate buffer with pH=3.0 and potential scan rate of 100.0 mV s<sup>-1</sup>.

and 30.0-120.0 μM. The equation of linear least square calibration curve for the concentration range of 2.0-30.0 μM is:  $I(\mu\text{A}) = 0.8074 \times C_{\text{HMX}} + 5.0582$  ( $R^2 = 0.9948$ ), with the experimental detection limit of 0.2 μM.

Relative standard deviation (RSD) of <2.5% for 10.0 μM HMX (for 5 analysis) showed a suitable reproducibility.

Compared to the conventional chromatographic and colorimetric, the proposed method having lengthy and tedious extraction procedures, is relatively fast, with high sensitivity and simplicity. HMX explosives show an extremely weak reduction current signal in water samples [2]. Comparison between the sensing performance of the AgNPs/MWCNTs based sensor and the previous electrochemical sensors of HMX shows that the reduction potential of HMX (related to electrocatalytic performance) is almost -0.3 to -0.5 V (vs. SCE) lower than other voltammetry methods [9, 13], that it can essentially reduce the interference effects of other reducible compounds. Also, this proposed method shows two linear dynamic ranges of 2.0-30.0 and 30.0-120.0 μM with the experimental LOD of 0.2 μM for HMX, which exhibits comprehensive advantages for the determination of HMX in water and soil samples. Other reported sensors such as SWV on GCE in toxic acetonitrile solution and expensive tetrabutylammonium bromide supporting electrolyte show a LOD of 3.38 μM with the linear range of 165.6-615.2 μM [9]. Also, a method reported by cyclic voltammetry on the boron-doped graphene indicates relatively comparable analytical figures with a LOD of 0.83 μM and linear range of 2.0-100.0 μM [13], but with lower electrocatalytic performance or significantly higher reduction potential for HMX. Also, in the present report, the interference of some cations and anions on the voltammetry determination of 10.0 μM HMX was evaluated. 800-fold of Na<sup>+</sup>, K<sup>+</sup>, Ca<sup>2+</sup>, Mg<sup>2+</sup>, NH<sub>4</sub><sup>+</sup>, Cl<sup>-</sup>, SO<sub>4</sub><sup>2-</sup>, NO<sub>3</sub><sup>-</sup>, 20-fold of Fe<sup>3+</sup> have almost no influence (less than 5.0%) on the current response of HMX. Interestingly, conventional NO<sub>3</sub><sup>-</sup> salts do not significantly affect the detection of HMX, but other electrochemically reducible hazardous materials such as trinitrotoluene (TNT) and RDX can interfere.

### 3.7. Application

The performance of the proposed method was assessed in some groundwater and soil samples by adding the standard value of HMX to them. The calibration method of standard addition was used for the analysis of prepared samples. The data given in **Table 1** show satisfactory results for the analytical determination of HMX in real samples.

## 4. Conclusions

In summary, an AgNPs/MWCNTs/GCE sensor was developed for electrocatalytic reduction and

determination of HMX explosive in water samples. The two-stage electrochemical reduction of this material is significantly facilitated on the electrode containing Ag nanoparticles compared to bare carbon nanotubes. The reduction potential of HMX starts from -0.7 on AgNPs/MWCNTs to -0.30 V on bare MWCNTs, with an electron exchange rate constant of  $1.12 \pm 0.1 \text{ s}^{-1}$  and  $0.17 \pm 0.1 \text{ s}^{-1}$ , respectively, indicating the unique electrocatalytic properties of silver nanoparticles, and also accumulation properties of carbon nanotubes. Also, chronocoulometric studies showed that the reduction mechanism of HMX is two electrons transform with the transfer coefficient ( $\alpha$ ) of 0.14. The apparent diffusion coefficient ( $D$ ) was obtained by the chronoamperometry method was near  $2.01 \times 10^{-4} \text{ cm}^2 \text{ s}^{-1}$ , and the catalytic rate constant of HMX on AgNPs/MWCNTs nanocomposite is 7.48 times higher than that of bare MWCNTs, confirmed by LSV method and Tafel plots. The performance of the proposed method was evaluated in some groundwater and soil samples, with an experimental detection limit of 0.2  $\mu\text{M}$  HMX using the cyclic voltammetry technique.

### Acknowledgements

The authors are grateful for the financial support of this work by Malek-ashtar University of Technology (I.R. Iran).

### References

- [1] J.P. Agrawal, High energy materials: propellants, explosives and pyrotechnics. John Wiley & Sons (2010).
- [2] M. Galik, A.M. O'Mahony, J. Wang, Electroanalysis. 23 (2011) 1193–1204.
- [3] S. Damiri, S. Namvar, H. Panahi, Def. Technol. 13 (2017) 392–396.
- [4] H.R. Pouretedal, S. Damiri, A. Shahsavan, Def. Technol. 14 (2018) 59–63.
- [5] U.S.A. ARDEC, MIL-DTL-45444C, Detail Specification, HMX: Cyclotetramethylene tetranitramine (1996).
- [6] C.P. Achuthan, C.I. Jose, Propellants, Explos. Pyrotech. 15 (1990) 271–275.
- [7] E.C. Mattos, E.D. Moreira, R.C.L. Dutra, M.F. Diniz, A.P. Ribeiro, K. Iha, Determination of the HMX and RDX content in synthesized energetic material by HPLC, FT-MIR, and FT-NIR spectroscopies, in: Quim. Nova (2004).
- [8] X. Pan, K. Tian, L.E. Jones, G.P. Cobb, Talanta. 70 (2006) 455–459.
- [9] N. Pon Saravanan, S. Venugopalan, N. Senthilkumar, P. Santhosh, B. Kavita, H. Gurumallesh Prabu, Talanta. 69 (2006) 656–662.
- [10] S. Babae, A. Beiraghi, Anal. Chim. Acta. 662 (2010) 9–13.
- [11] A. Üzer, Z. Can, İ. Akin, E. Erçağ, R. Apak, Anal. Chem. 86 (2014) 351–356.
- [12] T. Lu, Y. Yuan, X. He, M. Li, X. Pu, T. Xu, Z. Wen, RSC Adv. 5 (2015) 13021–13027.
- [13] Y. Xu, W. Lei, Z. Han, T. Wang, M. Xia, Q. Hao, Electrochim. Acta. 216 (2016) 219–227.
- [14] B. Rezaei, S. Damiri, J. Hazard. Mater. 183 (2010) 138–144.
- [15] M. Nosuhi, A. Nezamzadeh-Ejehieh, Electrochim. Acta. 223 (2017) 47–62.
- [16] A. Ehsani, R. Asgari, A. Rostami-Vartooni, H.M. Shiri, A. Yeganeh-Faal, Iran. J. Catal. 6 (2016) 269–274.
- [17] B. Rezaei, S. Damiri, Talanta. 83 (2010) 194–204.
- [18] B. Rezaei, S. Damiri, IEEE Sens. J. 8 (2008) 1523–1529.
- [19] B. Rezaei, S. Damiri, Electrochim. Acta. 55 (2010) 1801–1808.
- [20] T. Tamiji, A. Nezamzadeh-Ejehieh, J. Taiwan Inst. Chem. Eng. 104 (2019) 130–138.
- [21] V. Bansal, V. Li, A.P. O'Mullane, S.K. Bhargava, Cryst. Eng. Comm. 12 (2010) 4280–4286.
- [22] S. Damiri, H.R. Pouretedal, A. Heidari, Int. J. Environ. Anal. Chem. 96 (2016) 1059–1073.
- [23] A.J. Bard, L.R. Faulkner, Electrochemical Methods: Fundamentals and Applications, 2nd Edition, John Wiley & Sons (2002).
- [24] M.O. Turcotte-Savard, S. Brochu, Soil Sediment Contam. 28 (2019) 245–257.
- [25] J.M. Linge, H. Erikson, A. Kasikov, M. Rähn, V. Sammelselg, K. Tammeveski, Electrochim. Acta. 325 (2019) 134922–134927.
- [26] T. Tamiji, A. Nezamzadeh-Ejehieh, J. Electroanal. Chem. 829 (2018) 95–105.
- [27] N. Raeisi-Kheirabadi, A. Nezamzadeh-Ejehieh, H. Aghaei, Microchem. J. 162 (2021) 105869–105874.
- [28] A. Mirzaie, R. Hamidi, F. Hamidi, Iran. J. Catal. 5 (2015) 275–283.
- [29] J.C. Lynch, J.M. Brannon, J.J. Delfino, Chemosphere. 47 (2002) 725–734.
- [30] S. Sharifian, A. Nezamzadeh-Ejehieh, Mater. Sci. Eng. C 58 (2016) 510–520.
- [31] N. Raeisi-Kheirabadi, A. Nezamzadeh-Ejehieh, H. Aghaei, Iran. J. Catal. 11 (2021) 181–189.